DMD Fast Forward. Published on May 12, 2021 as DOI: 10.1124/dmd.121.000359
This article has not been copyedited and formatted. The final version may differ from this version.

Hepatic Scaling Factors for In Vitro-In Vivo Extrapolation (IVIVE) of Metabolic Drug Clearance in Patients with Colorectal Cancer with Liver Metastasis

Areti-Maria Vasilogianni, Brahim Achour, Daniel Scotcher, Sheila Annie Peters, Zubida M. Al-Majdoub, Jill Barber, Amin Rostami-Hodjegan

Centre for Applied Pharmacokinetic Research, Division of Pharmacy and Optometry, School of health Sciences, University of Manchester, Manchester, M13 9PT, UK (A.M.V., B.A., D.S., Z.M.A., J.B., A.R.-H.).

Translational Quantitative Pharmacology, BioPharma, R&D Global Early Development, Merck KGaA, Frankfurter Str. 250, F130/005, 64293 Darmstadt, Germany (S.A.P.).

Certara Inc (Simcyp Division), 1 Concourse Way, Sheffield, UK (A.R.-H.).

DMD Fast Forward. Published on May 12, 2021 as DOI: 10.1124/dmd.121.000359
This article has not been copyedited and formatted. The final version may differ from this version.

Running title: Hepatic scaling factors for CL in colorectal cancer

Keywords: MPPGL, CPPGL, Liver Homogenate, IVIVE, PBPK, Pharmacokinetics in Cancer

Corresponding author: Amin Rostami-Hodjegan; Centre for Applied Pharmacokinetic Research, School of Health Sciences, The University of Manchester, Stopford Building, Oxford Road, Manchester, M13 9PT, UK; Phone: +44 (0) 1613060634; E-mail address: amin.rostami@manchester.ac.uk

Number of text pages: 34

Number of Tables: 1

Number of Figures: 6

Number of References: 38

Number of words in Abstract: 242

Number of words in Introduction: 643

Number of words in Discussion: 1500

Abbreviations: AAG, Alpha-1-acid glycoprotein; BCA, bicinchoninic acid; BMI, body mass index; CPPGL, cytosolic protein per gram of liver; CRLM, colorectal cancer liver metastasis; HomPGL, homogenate protein per gram of liver; IVIVE, *in vitro* to *in vivo* extrapolation; MPPGL, microsomal protein per gram of liver; PBPK, physiologically based pharmacokinetics.

DMD Fast Forward. Published on May 12, 2021 as DOI: 10.1124/dmd.121.000359
This article has not been copyedited and formatted. The final version may differ from this version.

Abstract

In vitro-in vivo extrapolation (IVIVE) linked with physiologically based pharmacokinetic (PBPK) modelling is used to predict the fates of drugs in patients. Ideally, the IVIVE-PBPK models should incorporate "systems" information accounting for characteristics of the specific target population. There is a paucity of such scaling factors in cancer, particularly microsomal protein per gram of liver (MPPGL) and cytosolic protein per gram of liver (CPPGL). In this study, cancerous and histologically normal liver tissue from 16 patients with colorectal liver metastasis (CRLM) were fractionated to microsomes and cytosol. Protein content was measured in homogenates, microsomes and cytosol. The loss of microsomal protein during fractionation was accounted for using corrections based on NADPH cytochrome P450 reductase activity in different matrices. MPPGL was significantly lower in cancerous tissue (24.8 ± 9.8 mg/g) than histologically normal tissue (39.0 ± 13.8 mg/g). CPPGL in cancerous tissue was 42.1 ± 12.9 mg/g compared with 56.2 ± 16.9 mg/g in normal tissue. No correlations between demographics (sex, age and BMI) and MPPGL or CPPGL were apparent in the data. The generated scaling factors together with assumptions regarding the relative volumes of cancerous versus non-cancerous tissue were used to simulate plasma exposure of drugs with different extraction ratios. The PBPK simulations revealed a substantial difference in drug exposure (AUC), up to 3.3-fold, when using typical scaling factors (healthy population) instead of disease-related parameters in cancer population. These indicate the importance of using population-specific scalars in IVIVE-PBPK for different disease states.

DMD Fast Forward. Published on May 12, 2021 as DOI: 10.1124/dmd.121.000359
This article has not been copyedited and formatted. The final version may differ from this version.

Significance statement

Accuracy in predicting the fate of drugs from in vitro data using IVIVE-PBPK depends on using correct scaling factors. The values for two of such scalars, namely microsomal and cytosolic protein per gram of liver, is not known in cancer patients. This study presents, for the first time, scaling factors from cancerous and matched histologically normal livers. PBPK simulations of various metabolically cleared drugs demonstrate the necessity of population-specific scaling for model-informed precision dosing in oncology.

DMD Fast Forward. Published on May 12, 2021 as DOI: 10.1124/dmd.121.000359
This article has not been copyedited and formatted. The final version may differ from this version.

Introduction

Cancer is a multifaceted disease characterized by deregulated cell growth with the potential to invade tissues and form metastases. Colorectal cancer is the third most common type of cancer and is associated with the second highest number of deaths caused by cancer (Bray et al., 2018). Metastasis to the liver constitutes one of the main causes of mortality in patients with colorectal cancer (Siegel et al., 2018) as it accounts for 70% of metastases from colorectal cancer, followed by metastasis to the lungs, distant lymph nodes, and peritoneum (Holch et al., 2017). Metastasis to the liver can affect hepatic function as the resultant lesions occupy space in liver tissue leading to abnormal liver function tests (Jiang et al., 2018). Inflammation is a condition that may also affect the hepatic function, as inflammatory markers have been shown to be associated positively with the size of metastases (Wong et al., 2007).

Challenges in the development of new drugs in the area of oncology include the difficulty of recruiting from the appropriate patient population and safety issues when testing anti-cancer drugs of high toxicity in healthy volunteers (Gutierrez et al., 2009; Bates et al., 2015). Given these challenges, and the high medical need, model-informed precision dosing (MIDD) and, in particularly, physiologically based pharmacokinetics (PBPK) are widely employed (Darwich et al., 2017). PBPK modelling has generally higher regulatory acceptance in the development of anti-cancer drugs than other disease areas (Yoshida et al., 2017), and models are used to inform dosing of cancer patients.

In vitro-in vivo extrapolation (IVIVE) employs models that incorporate “systems” information and in vitro drug data to predict plasma and tissue concentration-time profiles, which are critical components of bottom-up PBPK models (Rostami-Hodjegan, 2012). Data

obtained using population-specific in vitro systems taking into account potential differences in functional activity need to be scaled to in vivo outcomes. For IVIVE of hepatic drug clearance, different in vitro systems can be used, including recombinantly expressed enzymes, hepatocytes, liver microsomes and cytosol. The scalars related to liver microsomes and cytosol are microsomal protein per gram of liver (MPPGL) and cytosolic protein per gram of liver (CPPGL), respectively (Barter et al., 2007).

To obtain microsomal and cytosolic fractions required for in vitro data, it is necessary to homogenize liver tissue and fractionate the homogenate using differential centrifugation. During tissue fractionation, membrane protein is subject to significant losses (Wilson et al., 2003). Accounting for protein losses is necessary for obtaining correct MPPGL values and thus, more accurate clearance predictions. For the correction of microsomal protein loss, different microsomal markers can be used, such as NADPH cytochrome P450 reductase or total P450 content measured in the homogenate and microsomal fractions (Barter et al., 2008). Cytosolic markers for the correction of cytosolic protein loss include alcohol dehydrogenase and glutathione-S-transferase (Cubitt et al., 2011); however, loss of cytosolic protein is expected to be negligible (soluble fraction). MPPGL and CPPGL values have been reported in healthy human liver with mean values of 32 mg/g liver and 80.7 mg/g liver, respectively (Barter et al., 2007; Cubitt et al., 2011).

Although scalars have been reported for healthy liver, such data are scarce in disease populations, such as cancer. Available scalar data in liver cancer suggest that MPPGL is different in livers with hepatocellular carcinoma relative to normal liver tissue (Zhang et al., 2015; Gao et al., 2016). To our knowledge, there are no reports of scalars or IVIVE-PBPK models for colorectal liver metastasis (CRLM) for the prediction of in vivo hepatic drug clearance. The aim of this study was to generate MPPGL and CPPGL scaling factors in

DMD Fast Forward. Published on May 12, 2021 as DOI: 10.1124/dmd.121.000359
This article has not been copyedited and formatted. The final version may differ from this version.

cancerous liver tissue from CRLM patients and compare the values with scalars from matched histologically normal tissue. The scalars were applied in PBPK simulations to predict in vivo hepatic clearance. This study highlights the importance of applying appropriate population-specific scalars for IVIVE of metabolic drug clearance in CRLM patients.

DMD Fast Forward. Published on May 12, 2021 as DOI: 10.1124/dmd.121.000359
This article has not been copyedited and formatted. The final version may differ from this version.

Materials and Methods

Materials and chemicals

All chemicals were purchased from Sigma-Aldrich (Poole, Dorset, UK) unless otherwise stated. EDTA-free protease inhibitor cocktail was obtained from Roche Applied Sciences (Mannheim, Germany).

Liver samples

Matched cancerous and histologically normal liver tissue specimens from 16 adult CRLM patients were obtained opportunistically following hepatectomy from the Manchester University NHS Foundation Trust (MFT) Biobank, Manchester, UK. The study was covered under the MFT Biobank generic ethics approval (NRES 14/NW/1260 and 19/NW/0644). Among the 16 donors, 7 were female and 9 were male, and their ages ranged from 34 to 85 years. The body mass index (BMI) of the patients ranged from 21.6 to 36.3 kg/m^2. Supplemental Table 1 presents demographic and clinical details of the donors.

Preparation of human liver microsomal and cytosolic fractions

Microsomal and cytosolic fractions were generated from liver tissue using differential centrifugation as previously described (Achour et al., 2017). Liver tissue was homogenized by a mechanical homogenizer (Thermo Fisher Scientific, UK) in homogenization buffer (150 mM KCl, 2 mM EDTA, 50 mM Tris, 1 mM dithiothreitol, and EDTA-free protease inhibitor cocktail, pH 7.4) at 10 ml for each gram of liver tissue. The homogenate was centrifuged at 10,000 *g* for 20 min at 4°C using an Optima^{TM} L-100 ultracentrifuge (Beckman Coulter, Fullerton, CA). The first pellet (cell debris) was stored at -80°C and then the supernatant was further centrifuged at 100,000 *g* for 75 min at 4 °C. The cytosol (the supernatant) was stored

DMD Fast Forward. Published on May 12, 2021 as DOI: 10.1124/dmd.121.000359
This article has not been copyedited and formatted. The final version may differ from this version.

at -80°C and the pellet (microsomes) was re-suspended in 1 ml of storage buffer (0.25 M potassium phosphate, pH 7.25) per gram of liver tissue and stored at -80°C.

Measurement of total protein content in homogenates and fractions

The protein content of liver homogenates, microsomes and cytosolic samples was measured using bicinchoninic acid (BCA) protein assay (Pierce® Microplate BCA Protein Assay Kit – Reducing Agent Compatible) in triplicate. Absorbance was measured at 562 nm using a SpectraMax 190 platereader (Molecular Devices, Sunnyvale, CA) with bovine serum albumin used as calibration standard. For the homogenates and the cytosolic samples that contained dithiothreitol, a compatibility reagent solution was used. The cytosolic protein per gram of liver (CPPGL), and the homogenate protein per gram of liver (HomPPGL) were calculated based on the total protein content, and no further correction for loss was required.

Measurement of NADPH cytochrome P450 reductase activity

In the current study, NADPH P450 reductase activity was used to account for microsomal membrane loss during fractionation. The activity of NADPH P450 reductase was measured in homogenates and microsomes from the same liver samples in order to estimate loss of microsomal protein during fractionation. The protocol was adapted from methods by Guengerich et al. (2009) and Achour et al. (2011). In a 1 ml cuvette, oxidised equine cytochrome c (0.5 mM, 80 µL) was mixed with potassium phosphate buffer (0.25 M, 980 µl, pH 7.25), KCN (1 mM, 10 µl) and homogenates (10 µl, equivalent to 1 mg of tissue) or 1:10 diluted microsomes (10 µl, equivalent to 1 mg of tissue). The absorbance of the mixtures was measured using a Jenway 7315 UV-Visible spectrophotometer (Thermo Fisher Scientific) at 550 nm in kinetic mode. The absorbance was monitored for 2 min to establish the baseline, followed by addition of reduced NADPH solution (10 mM, 10 µl) to start the reaction of cytochrome c reduction, which was monitored for 5 min.

DMD Fast Forward. Published on May 12, 2021 as DOI: 10.1124/dmd.121.000359
This article has not been copyedited and formatted. The final version may differ from this version.

The slope of the initial linear phase of the reaction is directly proportional to the amount of cytochrome P450 reductase in the sample. The enzyme activity (units/mg liver tissue) was calculated using Equation 1 and fractional loss of microsomal protein was estimated based on the ratio of activity in microsomes relative to the homogenate from the same liver sample (Equation 2), using the ratio of the slope from the microsomal fraction (1 mg of tissue) to the slope from the homogenate (1 mg of total protein) for each individual. The ratios also allowed calculation of microsomal membrane enrichment. MPPGL for each sample was corrected using the recovery factors according to Equation 3 (Barter et al., 2008). Recovery factor is equal to 1-fractional loss of microsomal protein.

$$Enzyme\ activity = \frac{\Delta A_{550}/min \times dil \times total\ volume}{21.1 \times V}$$ (Equation 1)

ΔA550/min: rate of change in the absorbance at 550 nm

dil: dilution factor of the original enzyme sample

Total volume: volume of the reaction mixture (ml)

21.1 is the extinction coefficient for reduced cytochrome c ($mM^{-1}\ cm^{-1}$)

V: volume of the enzyme sample (ml), corresponding to 1 mg of liver tissue

$$Microsomal\ loss = 1 - \frac{activity\ in\ microsomes}{activity\ in\ homogenate}$$ (Equation 2)

$$MPPGL\ (mg\ g^{-1}) = \frac{Yield\ of\ microsomal\ protein\ (mg\ g^{-1})}{1 - Fraction\ loss\ of\ microsomal\ protein}$$ (Equation 3)

Statistical data analysis

Statistical data analysis was performed and graphs were generated using GraphPad Prism 8.1.2 (La Jolla, California USA). The data is presented as mean ± standard deviation (SD). Coefficient of variation (CV) was used to describe variability in datasets and the Kolmogorov-Smirnov test was used to assess the normality of distribution of the datasets.

DMD Fast Forward. Published on May 12, 2021 as DOI: 10.1124/dmd.121.000359
This article has not been copyedited and formatted. The final version may differ from this version.

Several datasets did not follow normal distribution, and therefore non-parametric statistical tests for differences were used. Differences in HomPPGL, uncorrected MPPGL and CPPGL values between histologically normal and matched cancerous tissues were assessed using Wilcoxon test. Differences in MPPGL values between histologically normal and matched cancerous tissues were assessed using Mann-Whitney test. This test was also used for the assessment of the effect of hepatic lobe of origin and sex of donors on MPPGL and CPPGL in normal and cancerous tissues. For the assessment of the effect of BMI and age on MPPGL and CPPGL, Spearman correlation and linear regression analysis were used. In each of the above cases, the probability cut-off value for statistical significance was set at 0.05.

Physiologically based pharmacokinetic (PBPK) simulations

The effect of using the generated scaling factors in a cancer population was assessed using PBPK modelling on Simcyp V18 Release 1 (Certara, Sheffield, UK) in healthy and cancer populations. For the assessment of effects of MPPGL changes on simulated plasma drug exposure, four cytochrome P450 substrates with different hepatic extraction ratios (see Table 1) were used: alfentanil (predominantly metabolized by CYP3A4), alprazolam (predominantly metabolized by CYP3A4 and CYP3A5), midazolam (predominantly metabolized by CYP3A4 and CYP3A5), and desipramine (predominantly metabolized by CYP2D6). CYP isoforms are responsible for the metabolism of the majority of clinically used drugs in all fields of treatment (anti-cancer and non-anti-cancer drugs), with CYP3A4/5 being the most prevalent, followed by CYP2D6. For this reason, we used CYP3A4, CYP3A5 and CYP2D6 enzymes for our simulations. The compound files were not changed from those provided within the Simcyp simulator. PBPK simulations were performed using system parameters already available on the simulator for healthy (“Sim-Healthy Volunteers”) and cancer (“Sim-Cancer”) virtual populations, without or with inclusion of MPPGL data

DMD Fast Forward. Published on May 12, 2021 as DOI: 10.1124/dmd.121.000359
This article has not been copyedited and formatted. The final version may differ from this version.

measured in current study. The effects of MPPGL changes in cancer on drug exposure following oral administration were assessed using four different MPPGL models:

MPPGL model 1 (Healthy; Healthy population): the default MPPGL in Simcyp was used for the healthy population; mean MPPGL was 39.8 mg/g tissue (defined by the Simcyp model), (Equation 4, Barter et al., 2008).

$$Mean\ MPPGL\ \left(\frac{mg}{g}\right) = 10\text{^}(1.407\ +\ 0.0158 * \text{Age}\ -\ 0.00038 * \text{Age\^2}\ +\ 0.000024 * \text{Age\^3})$$

(Equation 4), coefficient of variabilities (CV)% is 26.9

MPPGL model 2 (Cancer-D; Cancer-Default population): the default MPPGL in Simcyp was used for the cancer population; mean MPPGL was 39.8 mg/g tissue (defined by the Simcyp model), (Equation 4, Barter et al., 2008).

These two models were used to assess any effects on drug exposure between healthy and cancer populations without changing MPPGL values. The key differences in the systems parameters between Healthy and Cancer-D involve age distribution, haematocrit, Alpha-1-acid glycoprotein (AAG) and albumin levels.

MPPGL model 3 (New Cancer-ALN; New Cancer population-assuming liver is obtained from cancer patients but entire liver tissue is histologically normal, ALN = All Liver Normal): experimentally-derived MPPGL in histologically normal tissue was used for the cancer population; mean MPPGL was 39 mg/g tissue, (Equation 5, adapted from Barter et al., 2008 with revised baseline).

$Mean\ MPPGL\ \left(\frac{mg}{g}\right) = 10\text{^}(1.59106462)$ (Equation 5), CV% is 35.36

DMD Fast Forward. Published on May 12, 2021 as DOI: 10.1124/dmd.121.000359
This article has not been copyedited and formatted. The final version may differ from this version.

Model 3 assumes that the whole liver remains histologically normal, and this implies the maximum metabolic capacity of microsomal enzymes. CV% used for this model is experimentally-derived based on MPPGL in histologically normal tissue.

MPPGL model 4 (New Cancer-ALC; New Cancer population-assuming liver is obtained from cancer patients and entire liver tissue is histologically cancerous, ALC = All Liver Cancerous): experimentally-derived MPPGL in cancerous tissue was used for the cancer population; mean MPPGL was 24.8 mg/g tissue, (Equation 6, adapted from Barter et al., 2008 with revised baseline).

$Mean\ MPPGL\ \left(\frac{mg}{g}\right) = 10\text{^}(1.3944516)$ (Equation 6), CV% is 39.7

Model 4 assumes that the whole liver is cancerous and this implies the minimum metabolic capacity of microsomal enzymes. It also assumes that the liver mass does not change and that each pmol of enzyme has the same activity, irrespective of disease state. CV% used for this model is experimentally-derived based on MPPGL in cancerous tissue.

The size of the liver being normal is important, as this will define how much of the liver will be fully functional. If a proportion of liver is not normal, this may lead to decreased scaled intrinsic clearance, with effect on clearance being compound dependent. In cases of a surgical resection, clearance should be calculated based on healthy MPPGL and remnant liver size. Although surgical resection is the ideal solution for CRLM patients, this is not feasible for many patients that have to live with a liver with histologically normal and cancerous parts, with unchangeable liver size. Therefore, metabolic capacities of enzymes come from 2 different sources: histologically normal and cancerous liver (relative contributions of normal and cancerous parts are unknown in the current study). In this case, it is more appropriate to

DMD Fast Forward. Published on May 12, 2021 as DOI: 10.1124/dmd.121.000359
This article has not been copyedited and formatted. The final version may differ from this version.

use MPPGL for histologically normal tissue with the weight of the liver being histologically normal and MPPGL for cancerous tissue with the weight of the liver being cancerous.

For Equation 4, the age was plotted against MPPGL values for Healthy population; for both observed and predicted (Barter et al., 2008) values (Supplemental Figure 1). For each model and for each drug, a generic trial design was used, with the following characteristics. The age range of the cancerous donors is 34-85 and the age range in the virtual population is 20 - 50 years old, which consists a limitation of our study. However, this limitation wouldn't have any effect on the final observations, as the age range is kept consistent in all the models, and additionally, age-dependent MPPGL in cancer samples was not apparent (Figure 4D). The mean (for all 100 virtual subjects) systemic concentration (C_{sys})-time profiles were plotted and the area under the curve from time 0 to infinity ($AUC_{0\text{-}inf}$) and maximum plasma concentration (C_{max}) values were compared across the four MPPGL methods/ models (Table 1). Parameters used for PBPK simulations are listed in Supplemental Table 2. Oral doses for alfentanil, alprazolam, midazolam and desipramine are 0.043 mg/kg, 0.5 mg, 5 mg, and 50 mg respectively.

Lack of differences in CPPGL between normal and cancerous tissue (see Results) meant that significant effects on the clearance and systemic concentrations of drugs metabolized by cytosolic enzymes were not expected. Therefore, no PBPK simulations were performed to assess possible effects on pharmacokinetics of drugs metabolized by cytosolic enzymes.

DMD Fast Forward. Published on May 12, 2021 as DOI: 10.1124/dmd.121.000359
This article has not been copyedited and formatted. The final version may differ from this version.

Results

Protein content of liver homogenates and fractions

Total protein content was measured in homogenates, microsomes, and cytosols from histologically normal and matched cancerous (n = 16) liver samples (Figure 1; Supplemental Table 3). The mean HomPPGL was 126.1 ± 46.7 mg/g in histologically normal samples and 86.9 ± 50.2 mg/g in matched cancer samples (range: 75.1-266.7 and 37.1-204.8 mg/g, respectively). The mean CPPGL was 56.2 ± 16.9 mg/g in histologically normal samples and 42.1 ± 12.9 mg/g in cancer samples (range: 32.3-80.7 and 24.8-67.2 mg/g, respectively). There was no statistically significant difference in HomPPGL (Wilcoxon test, $p = 0.0654$) and CPPGL between histologically normal and cancerous samples (Wilcoxon test, $p = 0.0654$). The mean microsomal protein isolated from liver, before correction for membrane loss was 15.8 ± 3.9 mg/g in histologically normal samples and 6.5 ± 3.3 mg/g in matched cancer samples (8.8-22.8 and 2.6-15.2 mg/g, respectively), and a 2.4-fold statistically significant difference (Wilcoxon test, $p < 0.0001$).

NADPH cytochrome P450 reductase activity in homogenates and microsomes

Activity of NADPH cytochrome P450 reductase was used to assess recovery and enrichment of microsomal membrane. Activity measurements were made in homogenates and microsomal fractions of histologically normal (n = 16) and matched cancer samples (n = 11) (Figure 2A and Supplemental Table 4). Activity measurements in 5 tumorous samples were below the limit of quantitation and thus, only data for 11 tumorous samples are presented.

DMD Fast Forward. Published on May 12, 2021 as DOI: 10.1124/dmd.121.000359
This article has not been copyedited and formatted. The final version may differ from this version.

The mean enzymatic activity in homogenates was 2.36 ± 0.73 units/mg in histologically normal tissues, and 0.58 ± 0.37 units/mg of tissue in cancer samples (range: 0.8-3.58 and 0.14-1.42 units/mg, respectively). In microsomal fractions, activity was 1.03 ± 0.44 units/mg of tissue in histologically normal tissues and 0.18 ± 0.19 units/mg of tissue in cancer samples (range: 0.34-1.72 and 0.03-0.71 units/mg of tissue, respectively).

Enrichment and recovery of microsomal proteins relative to homogenates were calculated for histologically normal (n = 16) and matched cancerous samples (n = 11), as shown in Figure 2B and C, respectively. Mean enrichment was 3.5 ± 1.5 fold (range: 1.5-7.3) for histologically normal and 3.3 ± 1.4 (range: 1.4-5.7 fold) for cancerous samples. Microsomal protein recovery was 0.4 ± 0.2 (range: 0.2-0.8) for histologically normal and 0.3 ± 0.1 (range: 0.1-0.5), with minimal difference in mean recovery for the normal (0.4) and cancerous samples (0.3).

Corrected microsomal protein per gram of liver (MPPGL)

The MPPGL values were corrected using the recovery factors for histologically normal (n = 16) and cancer tissues (n = 11) (Figure 3). The mean corrected MPPGL was 39 ± 13.8 mg/g histologically normal tissue and 24.8 ± 9.8 mg/g cancerous tissue (range: 16.5-63.1 mg/g and 8.7-43.9 mg/g, respectively). MPPGL values were significantly lower in tumorous samples compared with histologically normal samples (Mann-Whitney test, $p = 0.0109$).

Effect of demographics on MPPGL values

The effects of anatomical origin of liver tissue (left or right liver lobe), sex, BMI and age on MPPGL values were tested for histologically normal and cancerous tissues (Figure 4). Some demographics information are not available for each sample. For example, the liver lobe (right or left) from which the sample has been taken is not available for 3 of the patients. Similarly, BMI is not available for 3 of the patients. Therefore, only 13 samples are used for

DMD Fast Forward. Published on May 12, 2021 as DOI: 10.1124/dmd.121.000359
This article has not been copyedited and formatted. The final version may differ from this version.

the correlation of liber lobe or BMI with MPPGL. The mean MPPGL was 38.7 ± 13.1 mg/g in histologically normal tissue from the left liver lobe (n = 4; 25.4-56.1 mg/g) and 37.0 ± 14.4 mg/g in histologically normal tissue from the right liver lobe (n = 9; 16.5-61.0 mg/g). By contrast, MPPGL was 29.4 ± 4.3 mg/g in cancerous tissue from the left liver lobe (n = 2; 26.3-32.4) and 22.4 ± 7.7 mg/g in cancerous tissue from the right liver lobe (n = 7; 8.7-32.7 mg/g). The difference in MPPGL from different lobes for histologically normal was not statistically significant (Mann-Whitney test, $p = 0.9399$). The statistical test was not applied to data from tumorous samples due to the low sample size from the left liver lobe (n = 2) (Figure 4A). The MPPGL was 38.3 ± 14.3 mg/g and 39.5 ± 14.3 mg/g for female (n = 7; 6.5-56.1 mg/g) and male (n = 9; 25.4-63.1 mg/g) donors of histologically normal tissue, respectively. MPPGL was 23.3 ± 7.2 mg/g and 26.0 ± 12.2 mg/g for female (n = 5; 12.9-32.7 mg/g) and male (n = 6; 8.7-43.9 mg/g) donors of cancerous tissues, respectively. No significant differences in MPPGL between male and female donors of histologically normal (Mann-Whitney test, $p = 0.8371$) and tumorous tissues were observed (Mann-Whitney test, $p > 0.9999$) (Figure 4B). There was no trend in MPPGL values with BMI (Spearman test, $p = 0.6338$) or age (Spearman test, $p = 0.8711$) (Figure 4C and D, respectively).

Effect of demographics on CPPGL values

The effects of anatomical origin of tissue (left or right liver lobe), sex, BMI and age on CPPGL values were tested for histologically normal and cancerous tissues (Figure 5). Some demographics information are not available for each sample. For example, the liver lobe (right or left) from which the sample has been taken is not available for 3 of the patients. Similarly, BMI is not available for 3 of the patients. Therefore, only 13 samples are used for the correlation of liber lobe or BMI with CPPGL. The mean CPPGL was 47.7 ± 11.1 mg/g in histologically normal tissue from the left liver lobe (n = 4; 33.9-57.7 mg/g) and 58.3 ± 18.8

DMD Fast Forward. Published on May 12, 2021 as DOI: 10.1124/dmd.121.000359
This article has not been copyedited and formatted. The final version may differ from this version.

mg/g in histologically normal tissue from the right lobe (n = 9; 32.3-80.7 mg/g). CPPGL was 45.2 ± 11.4 mg/g in cancerous tissue from the left liver lobe (n = 4; 30.8-54.6 mg/g) and 38.5 ± 11.5 mg/g in cancerous tissue from the right liver lobe (n = 9; 24.8-58.6 mg/g). There was no statistically significant difference in CPPGL from different lobes for histologically normal (Mann-Whitney test, $p = 0.3301$) or tumorous samples (Mann-Whitney test, $p = 0.6042$) (Figure 5A). The CPPGL was 61.4 ± 14.9 mg/g and 52.2 ± 18 mg/g for female (n = 7; 34.1-77.1 mg/g) and male (n = 9; 32.3-80.7 mg/g) donors of histologically normal tissue, respectively. CPPGL was 37.8 ± 12.4 mg/g and 45.5 ± 12.9 mg/g for female (n = 7; 24.8-54.8 mg/g) and male (n = 9; 30.8-67.2 mg/g) donors of cancerous tissues. There was no statistically significant difference in CPPGL between male and female donors of histologically normal (Mann-Whitney test, $p = 0.2991$) or tumorous tissues (Mann-Whitney test, $p = 0.1738$) (Figure 5B). There was no specific correlation between CPPGL values and BMI (Spearman test, $p = 0.2191$) or age (Spearman test, $p = 0.27415$) (Figure 5C and D, respectively).

Physiologically based pharmacokinetic (PBPK) simulations

Simulations for four different drugs (alfentanil, alprazolam, midazolam, desipramine) were performed using four different methods (Figure 6); Model 1 (Healthy) used default MPPGL (Simcyp) with a healthy population, Model 2 (Cancer-D) used default MPPGL with a cancer population, Model 3 (New Cancer-ALN) used MPPGL measured in this study in histologically normal tissue with a cancer population, and Model 4 (New Cancer-ALC) used MPPGL measured in this study in cancer tissue with a cancer population. Table 1 lists pharmacokinetic parameter values (T_{max}, C_{max}, and $AUC_{0\text{-}inf}$) for all simulations. C_{max} is the maximum drug concentration observed in plasma, and T_{max} is the time at which the highest drug concentration occurs after drug administration. $AUC_{0\text{-}inf}$ is the area under the plasma

DMD Fast Forward. Published on May 12, 2021 as DOI: 10.1124/dmd.121.000359
This article has not been copyedited and formatted. The final version may differ from this version.

drug concentration-time curve from time 0 to infinity. New Cancer-ALN assumes that the whole liver is histologically normal, whereas New Cancer-ALC assumes that the whole liver is cancerous. For alfentanil, $AUC_{0\text{-inf}}$ predicted using MPPGL of cancerous tissue (New Cancer-ALC) was approximately 3.3 fold higher of that obtained using default MPPGL (Simcyp) with a healthy population (Healthy), whereas for midazolam, alprazolam and desipramine, this value was approximately 1.4 fold higher.

Discussion

Scaling factors, including MPPGL and CPPGL, are used for IVIVE of data generated in in vitro systems to predict metabolic clearance of drugs (Wilson et al., 2003; Barter et al., 2007; Cubitt et al., 2011). Inter-individual variability of MPPGL has been reported previously (Wilson et al., 2003; Barter et al., 2008) and may explain part of the variation in metabolic clearance in the absence of genetic differences in the abundance and activity of enzymes in individuals. The data describing scalars in special populations and in disease states, such as cancer, are scarce. In addition, the effects of changes in these scalars (MPPGL, CPPGL) in cancer patients on metabolic clearance have not been investigated. As cancer is not a uniform disease (for example, drug metabolizing enzymes and transporters may vary in different cancer types), the effects in each cancer type should be addressed independently. Changes in MPPGL for primary hepatocellular carcinoma compared with histologically normal tissue have been reported (Zhang et al., 2015; Gao et al., 2016), but corresponding data for metastatic liver cancer are currently lacking. To our knowledge, our study is the first to describe scaling factors for CRLM.

In this study, CPPGL and HomPPGL values were measured as the total protein content of each fraction, while MPPGL was calculated by correcting for protein loss during fractionation using cytochrome P450 reductase activity, a microsomal membrane marker.

DMD Fast Forward. Published on May 12, 2021 as DOI: 10.1124/dmd.121.000359
This article has not been copyedited and formatted. The final version may differ from this version.

MPPGL values for histologically normal tissues (39.0 ± 13.8 mg/g of tissue) were consistent with the literature (Pelkonen et al., 1973; Wilson et al., 2003; Barter et al., 2007; Zhang et al., 2015), while values in cancerous tissues were significantly lower (24.8 ± 12.9 mg/g of tissue). A difference in the CV% was also observed between the histologically normal (CV% = 35) and the cancer tissues (CV% = 40). Higher CV% in cancer tissues may reflect the heterogeneity of cancer tissues or the different number of samples (smaller in cancer) that could increase the variability in cancer. The global reduction in microsomal protein content suggests that the abundance (pmol/g liver) of microsomal proteins, such as cytochrome P450 enzymes, in liver tissue may decrease in CRLM. Reported data on cytochrome P450 are limited to qualitative evidence that identify specific enzymes in histologically normal and tumorous tissues from CRLM patients (Lane et al., 2004) and therefore, future proteomics studies involving quantification of such enzymes would be valuable. Functional activity studies with probe substrates would also be useful but require larger samples than are available to us currently. CPPGL and HomPPGL values showed little difference between cancerous and histologically normal tissues, and CPPGL in histologically normal tissue (56.2 ± 16.9 mg/g of tissue) was consistent with the literature (45-134 mg/g) (Boogaard et al., 1996; Renwick et al., 2002; Mutch et al., 2007).

The potential effects of donor demographics (such as age, sex, BMI) and sampled liver lobe on MPPGL and CPPGL values were evaluated. Statistical analysis showed no relationship between the examined variables and changes in MPPGL and CPPGL values. Barter et al. (2007) performed a meta-analysis of literature data from 114 individuals and reported a relationship between age and MPPGL; values decreased with increasing age (40 mg/g liver for a 30 years old individual and 31 mg/g liver for a 60 years old individual). This effect of age on MPPGL had not been discernible in the component individual studies (Pelkonen et al., 1974; Lipscomb et al., 1998, 2003; Wilson et al., 2003; Hakooz et al., 2006). A more recent

study by Barter et al. (2008) showed that MPPGL values increased from childhood until the age of 28 years, then decreased thereafter. The small sample size and large underlying variability in the data of the present study meant that any correlation of MPPGL with age could not be delineated. Likewise, BMI did not affect MPPGL and CPPGL in either normal or cancerous tissues based on data from this study. There is no published literature on correlation between BMI and MPPGL or CPPGL in cancer. The sex of donors had no discernible effect on MPPGL or CPPGL in normal or cancerous tissues, consistent with earlier studies (Wilson et al., 2003; Schmucker et al., 1990). In addition, the liver lobe from which the tissues were sampled did not have an effect on MPPGL or CPPGL values from either normal or cancerous tissues. There are no reported data in the literature about regional differences in human liver, but studies in mice showed that microsomal P450 activity is variable in different lobes (Rudeck et al., 2018). Additionally, there was an effort to correlate the MPPGL values to the disease severity. No trend was observed, although the way that the samples were categorized according to the disease severity was not completely quantitative. This is a result of the small number of samples, and the lack of the information about the disease severity for all the patients.

The impact of applying different MPPGL values as scalars was studied using PBPK simulations on different drugs (alfentanil, alprazolam, midazolam, desipramine) metabolized by CYP enzymes with different extraction ratios. Generally, PK profiles of drugs are expected to differ in cancer populations compared with profiles in healthy subjects. In many cases, clearance of anti-cancer drugs decreases in cancer patients compared with healthy individuals (Piotrovsky et al., 1998; Houk et al., 2009; Hudachek et al., 2010) for various reasons, including co-morbidities, such as hepatic and renal impairment in cancer patients (Suri et al., 2015). Another possible reason may be changes in MPPGL or CPPGL and differences in the expression of enzymes and transporters (Gao et al., 2016; Billington et al.,

2018). Our data showed little difference in CPPGL between normal and cancerous tissues, but significantly lower MPPGL in cancer samples. Therefore, only the effect of MPPGL on drug pharmacokinetics was assessed in the simulations. MPPGL was used in other studies for scaling in hepatocellular carcinoma and glioblastoma (Gao et al., 2016; Li et al., 2017), and the present study is the first to assess the effect of changes in MPPGL in CRLM. The results for all the drugs showed that the MPPGL value affected drug exposure, suggesting that the proportion of the liver affected by cancer affects drug levels reaching the systemic circulation. More specifically, when the whole liver was assumed to be tumorous, higher systemic concentration was predicted compared with a histologically normal liver. Our simulations show that using appropriate MPPGL values for a certain population is important for the prediction of drug exposure; however, the applied MPPGL value should be accompanied by the percentage of cancerous liver in each patient. Although the percentage of cancerous liver is not known for the present study, it is common practice for major hepatectomy to resect up to 70% of the total liver for a sufficient liver function, including histologically normal and cancerous tissue (Hemming et al., 2003; Jiang et al, 2018). As a result, there may be a significant contribution of the tumour to the overall liver activity in CRLM patients. If we know the proportion of normal to cancerous tissue for an individual, then such data can be incorporated into the PBPK model. Otherwise, sensitivity and uncertainty analysis should be performed between two extreme cases (100% normal vs 100% cancerous) to establish worst-case scenario. It is important to clarify that the predicted PK profiles are not compared with clinical data, which are not available for CRLM patients. Therefore, our simulations are not indicative of which method is correct with observations, but they point out the assumption that MPPGL affect the PK in cancer patients. Further work is needed to verify this updated PBPK cancer population model against clinical data. PK may also depend on cancer stage, starting with a small amount of liver being affected (New

DMD Fast Forward. Published on May 12, 2021 as DOI: 10.1124/dmd.121.000359
This article has not been copyedited and formatted. The final version may differ from this version.

Cancer-ALN) resulting in a high amount of liver being cancerous (New Cancer-ALC). In this study, we assumed that the abundance of CYPs in CRLM was the same as for the generic healthy and cancer population in Simcyp. Although there are no published data on the abundance in CRLM, potential differences in the abundance of CYPs may have additive effects on the PK (Vasilogianni et al., in preparation).

In summary, this study assessed, for the first time, scaling factors specific for CRLM patients and showed significantly lower MPPGL in cancerous tissue compared with histologically normal tissue from CRLM patients. HomPPGL and CPPGL did not differ significantly between cancerous and histologically normal samples. Donor demographics (age, sex, BMI) and the anatomical origin of samples (liver lobe) had no effect on MPPGL and CPPGL values. PBPK simulations on drugs with different extraction ratios metabolized by CYPs revealed substantial difference in drug exposure, up to 3.3-fold, when comparing default scaling factors to population-specific scalars. It is therefore recommended that appropriate population-specific MPPGL values, accounting for percentage of liver/tumorous liver tissue, should be considered for prediction of drug exposure in cancer patients. Future studies should quantify enzyme abundance differences to improve understanding of metabolic drug clearance in cancer.

DMD Fast Forward. Published on May 12, 2021 as DOI: 10.1124/dmd.121.000359
This article has not been copyedited and formatted. The final version may differ from this version.

Acknowledgments

The authors would like to thank the Manchester University NHS Foundation Trust (MFT) Biobank, Manchester, UK, for access to liver samples.

Authorship Contributions

Participated in research design: Vasilogianni, Peters, Achour, Barber, Rostami-Hodjegan

Conducted experiments: Vasilogianni, Achour

Performed data analysis: Vasilogianni, Achour, Scotcher

Wrote or contributed to the writing of the manuscript: Vasilogianni, Achour, Scotcher, Peters, Al-Majdoub, Barber, Rostami-Hodjegan

DMD Fast Forward. Published on May 12, 2021 as DOI: 10.1124/dmd.121.000359
This article has not been copyedited and formatted. The final version may differ from this version.

References

Achour B, Al Feteisi H, Lanucara F, Rostami-Hodjegan A, and Barber J (2017) Global proteomic analysis of human liver microsomes: Rapid characterization and quantification of hepatic drug-metabolizing enzymes. *Drug Metab Dispos* **45**:666-675.

Achour B, Barber J, and Rostami-Hodjegan A (2011) Cytochrome P450 Pig Liver Pie: Determination of Individual Cytochrome P450 Isoform Contents in Microsomes from Two Pig Livers Using Liquid Chromatography in Conjunction with Mass Spectrometry. *Drug Metab Dispos* **39**:2130–2134.

Barter ZE, Bayliss M, Beaune P, Boobis A, Carlile D, Edwards R, Houston BJ, Lake B, Lipscomb J, and Pelkonen O, et al. (2007) Scaling Factors for the Extrapolation of In Vivo Metabolic Drug Clearance From In Vitro Data: Reaching a Consensus on Values of Human Micro-somal Protein and Hepatocellularity Per Gram of Liver. *Curr Drug Metab* **8**:33–45.

Barter ZE, Chowdry JE, Harlow JR, Snawder JE, Lipscomb JC, and Rostami-Hodjegan A (2008) Covariation of human microsomal protein per gram of liver with age: Absence of influence of operator and sample storage may justify interlaboratory data pooling. *Drug Metab Dispos* **36**:2405–2409.

Bates SE, Berry DA, Balasubramaniam S, Bailey S, LoRusso PM, and Rubin EH (2015) Advancing Clinical Trials to Streamline Drug Development. *Clin Cancer Res* **21**:4527–4535.

Billington S, Ray AS, Salphati L, Xiao G, Chu X, Humphreys WG, Liao M, Lee CA, Mathias

A, and Hop C, et al. (2018) Transporter expression in non-cancerous and cancerous liver tissue from subjects with hepatocellular carcinoma and chronic hepatitis C infection quantified by LC-MS/MS proteomics. *Drug Metab Dispos* **46**:189-96.

Boogaard PJ, Sumner SC-J, and Bond JA (1996) Glutathione Conjugation of 1,2:3,4-Diepoxybutane in Human Liver and Rat and Mouse Liver and Lungin Vitro. *Toxicol Appl Pharmacol* **136**:307–316.

Bray F, Ferlay J, Soerjomataram I, Siegel RL, Torre LA, and Jemal A (2018) Global cancer statistics 2018: GLOBOCAN estimates of incidence and mortality worldwide for 36 cancers in 185 countries. *CA Cancer J Clin* **68**:394–424.

Cubitt HE, Houston JB, and Galetin A (2011) Prediction of Human Drug Clearance by Multiple Metabolic Pathways: Integration of Hepatic and Intestinal Microsomal and Cytosolic Data. *Drug Metab Dispos* **39**:864–873.

Darwich AS, Ogungbenro K, Hatley OJ, and Rostami-Hodjegan A (2017) Role of pharmacokinetic modeling and simulation in precision dosing of anticancer drugs. *Transl Cancer Res* **6**:1512–1529.

Gao J, Zhou J, He XP, Zhang YF, Gao N, Tian X, Fang Y, Wen Q, Jia LJ, and Jin H, et al. (2016) Changes in cytochrome P450s-mediated drug clearance in patients with hepatocellular carcinoma in vitro and in vivo: A bottom-up approach. *Oncotarget* **7**:28612–28623.

Guengerich FP, Martin M V, Sohl CD, and Cheng Q (2009) Measurement of cytochrome P450 and NADPH–cytochrome P450 reductase. *Nat Protoc* **4**:1245–1251.

Gutierrez ME, Kummar S, and Giaccone G (2009) Next generation oncology drug development: opportunities and challenges. *Nat Rev Clin Oncol* **6**:259–265.

Hakooz N, Ito K, Rawden H, Gill H, Lemmers L, Boobis AR, Edwards RJ, Carlile DJ, Lake BG, and Houston JB (2006) Determination of a Human Hepatic Microsomal Scaling Factor for Predicting in Vivo Drug Clearance. *Pharm Res* **23**:533–539.

Hemming AW, Reed AI, Howard RJ, Fujita S, Hochwald SN, Caridi JG, Hawkins IF, and Vauthey JN (2003) Preoperative portal vein embolization for extended hepatectomy. *Ann Surg* **237**:686–693.

Holch JW, Demmer M, Lamersdorf C, Michl M, Schulz C, von Einem JC, Modest DP, and Heinemann V (2017) Pattern and Dynamics of Distant Metastases in Metastatic Colorectal Cancer. *Visc Med* **33**:70–75.

Houk BE, Bello CL, Kang D, and Amantea M (2009) A population pharmacokinetic meta-analysis of sunitinib malate (SU11248) and its primary metabolite (SU12662) in healthy volunteers and oncology patients. *Clin Cancer Res* **15**:2497–2506.

Hudachek SF, Eckhardt SG, Hicks B, and Gustafson DL (2010) Population pharmacokinetic model of PI88, a heparanase inhibitor. *Cancer Chemoth Pharmacol* **65**:743-753.

Jiang Z, Li C, Zhao Z, Liu Z, Guan X, Yang M, Li X, Yuan D, Qiu S, and Wang X (2018) Abnormal Liver Function Induced by Space-Occupying Lesions Is Associated with Unfavorable Oncologic Outcome in Patients with Colorectal Cancer Liver Metastases. *Biomed Res Int* **2018**:1–7.

Lane CS, Nisar S, Griffiths WJ, Fuller BJ, Davidson BR, Hewes J, Welham KJ, and Patterson LH (2004) Identification of cytochrome P450 enzymes in human colorectal metastases and the surrounding liver: A proteomic approach. *Eur J Cancer* **40**:2127–2134.

Li J, Wu J, Bao X, Honea N, Xie Y, Kim S, Sparreboom A, and Sanai N (2017) Quantitative and mechanistic understanding of AZD1775 penetration across human blood-brain

barrier in glioblastoma patients using an IVIVE-PBPK modeling approach. *Clin Cancer Res* **23**:7454–7466.

Lipscomb JC, Fisher JW, Confer PD, and Byczkowski JZ (1998) In Vitro t oin Vivo Extrapolation for Trichloroethylene Metabolism in Humans. *Toxicol Appl Pharmacol* **152**:376–387.

Lipscomb JC, Teuschler LK, Swartout JC, Striley CAF, and Snawder JE (2003) Variance of Microsomal Protein and Cytochrome P450 2E1 and 3A Forms in Adult Human Liver. *Toxicol Mech Methods* **13**:45–51.

Mutch E, Nave R, McCracken N, Zech K, and Williams FM (2007) The role of esterases in the metabolism of ciclesonide to desisobutyryl-ciclesonide in human tissue. *Biochem Pharmacol* **73**:1657–1664.

Pelkonen O, Kaltiala EH, Larmi TKI, and Kärki NT (1973) Comparison of activities of drug-metabolizing enzymes in human fetal and adult livers. *Clin Pharmacol Ther* **14**:840–846.

Pelkonen O, Kaltiala EH, Larmi TKI, and Kärki NT (1974) Cytochrome P-450-linked monooxygenase system and drug-induced spectral interactions in human liver microsomes. *Chem Biol Interact* **9**:205–216.

Piotrovsky VK, Huang ML, Van Peer A, and Langenaecken C (1998) Effects of demographic variables on vorozole pharmacokinetics in healthy volunteers and in breast cancer patients. *Cancer Chemother Pharmacol* **42**:221–228.

Renwick AB, Ball SE, Tredger JM, Price RJ, Walters DG, Kao J, Scatina JA, and Lake BG (2002) Inhibition of zaleplon metabolism by cimetidine in the human liver: in vitro studies with subcellular fractions and precision-cut liver slices. *Xenobiotica* **32**:849–862.

Rostami-Hodjegan A (2012) Physiologically based pharmacokinetics joined with in vitro-in vivo extrapolation of ADME: A marriage under the arch of systems pharmacology. *Clin Pharmacol Ther* **92**:50–61.

Schmucker DL, Woodhouse KW, Wang RK, Wynne H, James OF, McManus M, and Kremers P (1990) Effects of age and gender on in vitro properties of human liver microsomal monooxygenases. *Clin Pharmacol Ther* **48**:365–374.

Siegel RL, Miller KD, and Jemal A (2018) Cancer statistics, 2018. *CA Cancer J Clin* **68**:7–30.

Suri A, Chapel S, Lu C, and Venkatakrishnan K (2015) Physiologically based and population PK modeling in optimizing drug development: A predict-learn-confirm analysis. *Clin Pharmacol Ther* **98**:336–344.

Thai HT, Mazuir F, Cartot-Cotton S, and Veyrat-Follet C (2015) Optimizing pharmacokinetic bridging studies in paediatric oncology using physiologically-based pharmacokinetic modelling: Application to docetaxel. *Br J Clin Pharmacol* **80**:534–547.

Wilson ZE, Rostami-Hodjegan A, Burn JL, Tooley A, Boyle J, Ellis SW, and Tucker GT (2003) Inter-individual variability in levels of human microsomal protein and hepatocellularity per gram of liver. *Br J Clin Pharmacol* **56**:433–440.

Wong VKH, Malik HZ, Hamady ZZR, Al-Mukhtar A, Gomez D, Prasad KR, Toogood GJ, and Lodge JPA (2007) C-reactive protein as a predictor of prognosis following curative resection for colorectal liver metastases. *Br J Cancer* **96**:222–225.

Yoshida K, Budha N, and Jin JY (2017) Impact of physiologically based pharmacokinetic models on regulatory reviews and product labels: Frequent utilization in the field of oncology. *Clin Pharmacol Ther* **101**:597–602.

Zhang H, Gao N, Tian X, Liu T, Fang Y, Zhou J, Wen Q, Xu B, Qi B, and Gao J, et al. (2015) Content and activity of human liver microsomal protein and prediction of individual hepatic clearance in vivo. *Sci Rep* **5**:17671.

DMD Fast Forward. Published on May 12, 2021 as DOI: 10.1124/dmd.121.000359
This article has not been copyedited and formatted. The final version may differ from this version.

Footnotes

This work was supported by Merck KGaA, Frankfurter Str. 250, F130/005, 64293 Darmstadt, Germany.

A.R.-H. holds shares in Certara, a company focusing on Model-Informed Drug Development and declares no support from any organization for the submitted work. All other authors declare that they have no conflicts of interest.

DMD Fast Forward. Published on May 12, 2021 as DOI: 10.1124/dmd.121.000359
This article has not been copyedited and formatted. The final version may differ from this version.

Figure Legends

Figure 1. Total protein content (mg per gram of liver) in homogenates (HomPPGL, A), microsomal fractions (MPPGL before correction for losses, B) and cytosolic fractions (CPPGL, C) from histologically normal and matched tumor samples (n=16). The MPPGL values in panel B are not corrected for loss of membrane protein. Blue and red symbols represent normal and cancer samples. The lines represent means, error bars represent standard deviations, and percentages represent CVs. The asterisks (****) represent statistical differences with $p < 0.0001$ between histologically normal and cancerous tissues. Wilcoxon test was used for comparison of HomPPGL, uncorrected MPPGL, and CPPGL between matched cancerous and histologically normal samples.

Figure 2. Activity of NADPH cytochrome P450 reductase in homogenates and microsomes from histologically normal (n = 16) and tumor samples (n = 11) from CRLM patients (A). Each bar represent the mean value of triplicate measurements of each individual sample. Blue open and solid bars correspond to normal homogenates and microsomes, respectively. Red open and solid bars correspond to cancer homogenates and microsomes, respectively. Fold-enrichment (B) and recovery (C) of microsomal proteins from histologically normal (n = 16) and tumor (n = 13) samples from CRLM patients. Lines represent means, error bars represent standard deviations, and percentages represent CVs. Blue and red symbols represent histologically normal and tumor samples, respectively.

Figure 3. Corrected microsomal protein content (mg) per gram tissue (MPPGL) from histologically normal (n = 16) and tumor samples (n = 11). Lines represent means, error bars represent standard deviations, and percentages represent CVs. The asterisk (*) represent statistical difference (Mann-Whitney test, $p < 0.05$).

Figure 4. Effects of liver lobe (A), sex (B), BMI (C) and age (D) on MPPGL values for histologically normal and cancer samples. In panels A and B, lines represent means, error bars represent standard deviation values and percentages represent CVs. Mann-Whitney test was used to assess the effect of hepatic lobes and sex. Spearman correlation and linear regression were used to assess the effect of BMI and age. Blue symbols represent histologically normal samples and red symbols represent cancer samples. N.S. means no significant relation ($p > 0.05$).

Figure 5. Effects of liver lobe (A), sex (B), BMI (C) and age (D) on CPPGL values for histologically normal and cancer samples. In panels A and B, lines represent means, error bars represent standard deviation values and percentages represent CVs. Mann-Whitney test was used to assess the effect of hepatic lobes and sex. Spearman correlation and linear regression were used to assess the effect of BMI and age. Blue symbols represent histologically normal samples and red symbols represent cancer samples. N.S. means no significant relation ($p > 0.05$).

DMD Fast Forward. Published on May 12, 2021 as DOI: 10.1124/dmd.121.000359
This article has not been copyedited and formatted. The final version may differ from this version.

Figure 6. Mean predicted systemic concentration over time (24 hours) after oral administration of alfentanil (A), midazolam (B), alprazolam (C), and desipramine (D). For each drug, four different methods of scaling were used. Healthy: default MPPGL (Simcyp) with a healthy population. Cancer-D: default MPPGL with a cancer population. New Cancer-ALN: MPPGL measured in this study for histologically normal tissue with a cancer population. New Cancer-ALC: MPPGL measured in this study for cancer tissue with a cancer population. Inset graphs show the Relative $AUC_{0\text{-}inf}$ (0 to infinity) ratios of Cancer-D, New Cancer-ALN, and New Cancer-ALC to Healthy.

DMD Fast Forward. Published on May 12, 2021 as DOI: 10.1124/dmd.121.000359
This article has not been copyedited and formatted. The final version may differ from this version.

Tables

Table 1. Mean predicted E_H, Tmax, Cmax, and $AUC_{0\text{-inf}}$ for oral alfentanil, alprazolam, midazolam, and desipramine using four different scaling methods within PBPK model. $AUC_{0\text{-inf}}$ ratios using different methods are also provided.

Drug	Model	E_H	Cmax (ng/ml)	$AUC_{0\text{-inf}}$ (ng/ml.h)	Tmax (h)	Relative $AUC_{0\text{-inf}}$ ratios to Healthy
Alfentanil	Healthy	0.36	24	59	0.6	
	Cancer-D	0.24	33	120	0.9	2
	New Cancer-ALN	0.25	33	120	0.9	2
	New Cancer-ALC	0.17	39	193	0.9	3.3
Alprazolam	Healthy	0.04	8	144	1.2	
	Cancer-D	0.04	8	142	1.2	1
	New Cancer-ALN	0.04	8	140	1.2	1
	New Cancer-ALC	0.03	8	199	1.3	1.4
Midazolam	Healthy	0.43	24	76	0.6	
	Cancer-D	0.48	21	65	0.6	0.9
	New Cancer-ALN	0.48	21	65	0.5	0.9
	New Cancer-	0.38	27	104	0.6	1.4

DMD Fast Forward. Published on May 12, 2021 as DOI: 10.1124/dmd.121.000359
This article has not been copyedited and formatted. The final version may differ from this version.

	ALC					
Desipramine	Healthy	0.42	16	1385	5.9	
	Cancer-D	0.34	17	1421	5.9	1
	New Cancer-ALN	0.35	17	1406	5.9	1
	New Cancer-ALC	0.27	19	1989	6.4	1.4

Hepatic extraction ratio = E_H, Cmax = maximum plasma concentration, $AUC_{0\text{-}inf}$ = Area under the curve from time 0 to infinity, T_{max} = time at which C_{max} is observed. For each simulation, ten trials and ten subjects per trial were included.

Healthy: default MPPGL (Simcyp) with a healthy population. Cancer-D: default MPPGL with a cancer population. New Cancer-ALN: MPPGL measured in this study for histologically normal tissue with a cancer population. New Cancer-ALC: MPPGL measured in this study for cancer tissue with a cancer population.

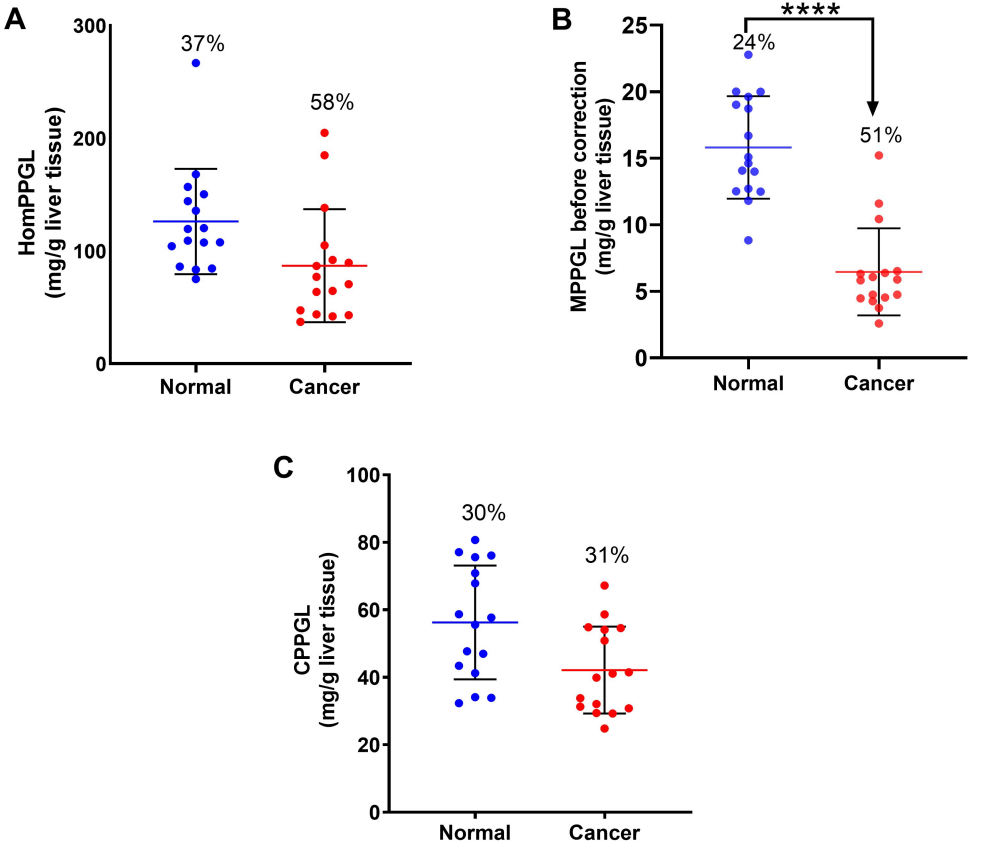
A
HomPPGL
(mg/g liver tissue)
300
200
100
0
37%
58%
Normal
Cancer
B
MPPGL before correction
(mg/g liver tissue)
25
20
15
10
5
0
****
24%
51%
Normal
Cancer
C
CPPGL
(mg/g liver tissue)
100
80
60
40
20
0
30%
31%
Normal
Cancer

Figure 1

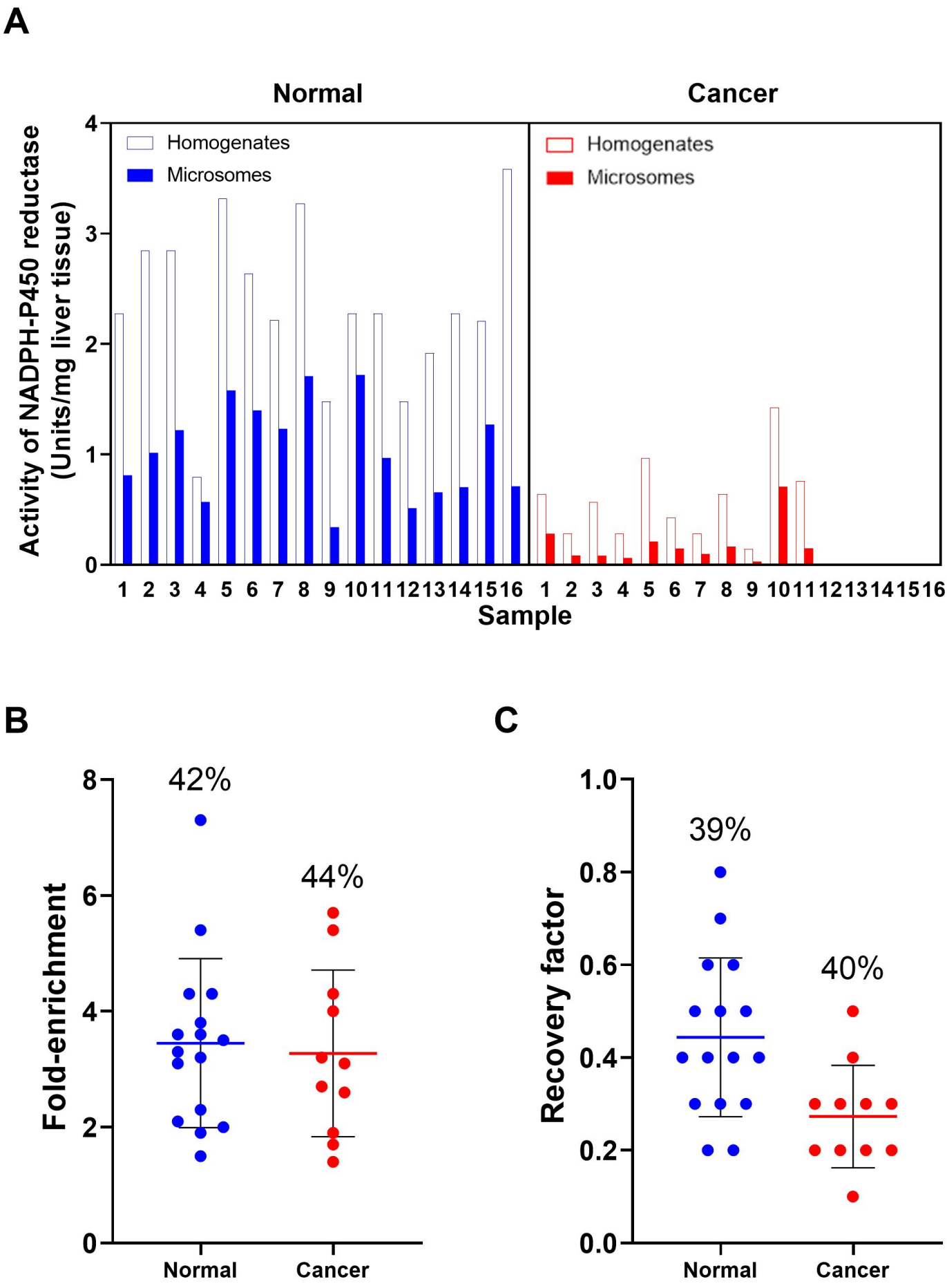
A
Normal
Cancer
Homogenates
Microsomes
Homogenates
Microsomes
Activity of NADPH-P450 reductase
(Units/mg liver tissue)
0
1
2
3
4
1 2 3 4 5 6 7 8 9 10 11 12 13 14 15 16 1 2 3 4 5 6 7 8 9 10 11 12 13 14 15 16
Sample
B
42%
44%
Fold-enrichment
0
2
4
6
8
Normal
Cancer
C
39%
40%
Recovery factor
0.0
0.2
0.4
0.6
0.8
1.0
Normal
Cancer

Figure 2

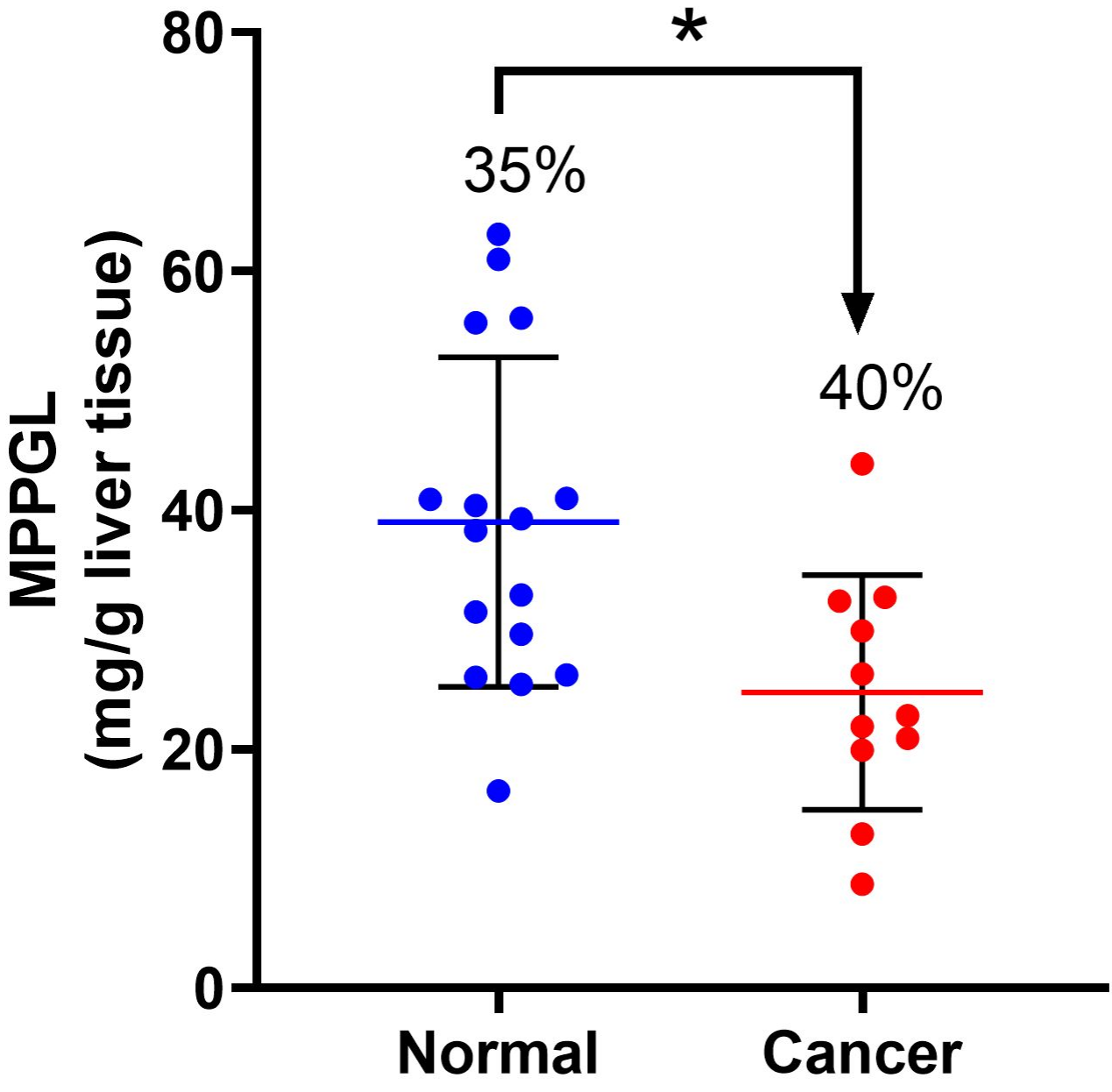

Figure 3

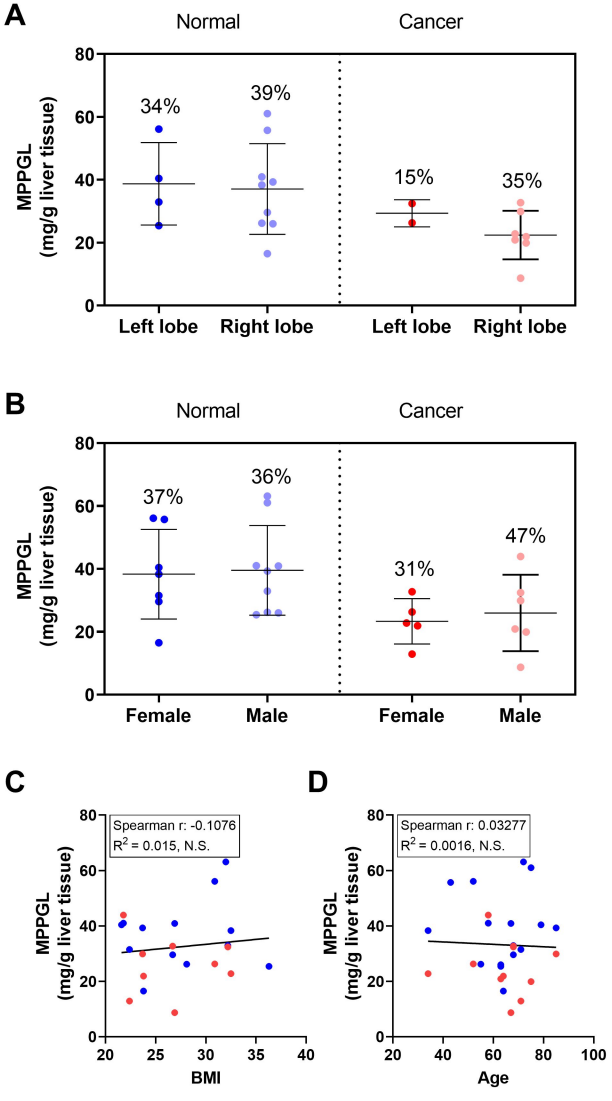
A
Normal
Cancer
MPPGL
(mg/g liver tissue)
80
60
40
20
0
34%
39%
15%
35%
Left lobe
Right lobe
Left lobe
Right lobe
B
Normal
Cancer
MPPGL
(mg/g liver tissue)
37%
36%
31%
47%
Female
Male
Female
Male
C
Spearman r: -0.1076
R2 = 0.015, N.S.
MPPGL
(mg/g liver tissue)
BMI
20
25
30
35
40
D
Spearman r: 0.03277
R2 = 0.0016, N.S.
MPPGL
(mg/g liver tissue)
Age
20
40
60
80
100

Figure 4

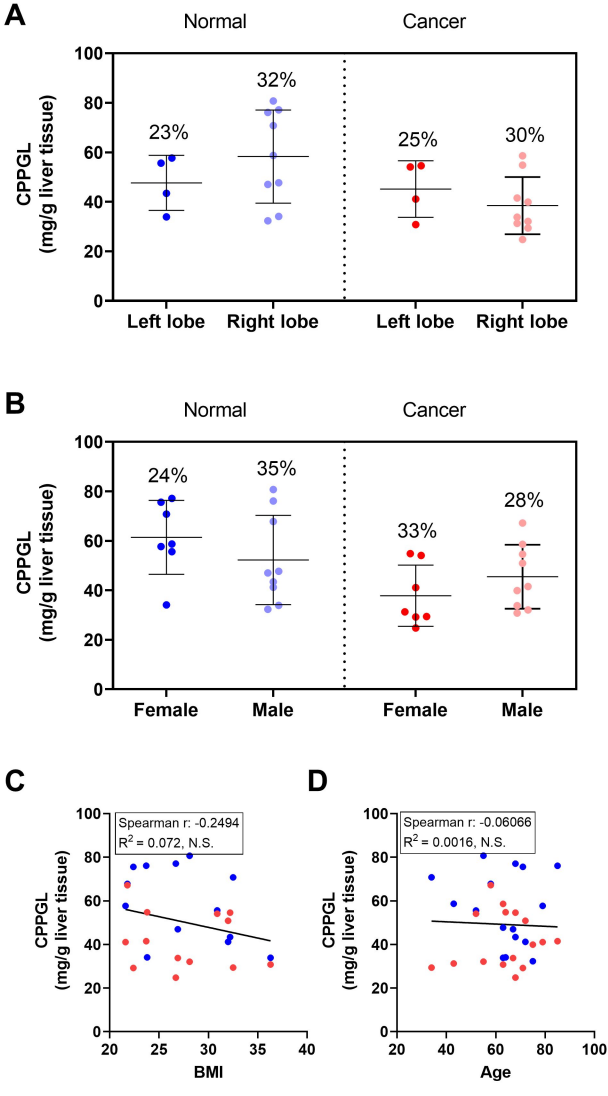
A
Normal
Cancer
CPPGL
(mg/g liver tissue)
100
80
60
40
20
0
23%
32%
25%
30%
Left lobe
Right lobe
Left lobe
Right lobe
B
Normal
Cancer
CPPGL
(mg/g liver tissue)
24%
35%
33%
28%
Female
Male
Female
Male
C
Spearman r: -0.2494
R2 = 0.072, N.S.
CPPGL
(mg/g liver tissue)
BMI
20
25
30
35
40
D
Spearman r: -0.06066
R2 = 0.0016, N.S.
CPPGL
(mg/g liver tissue)
Age
20
40
60
80
100

Figure 5

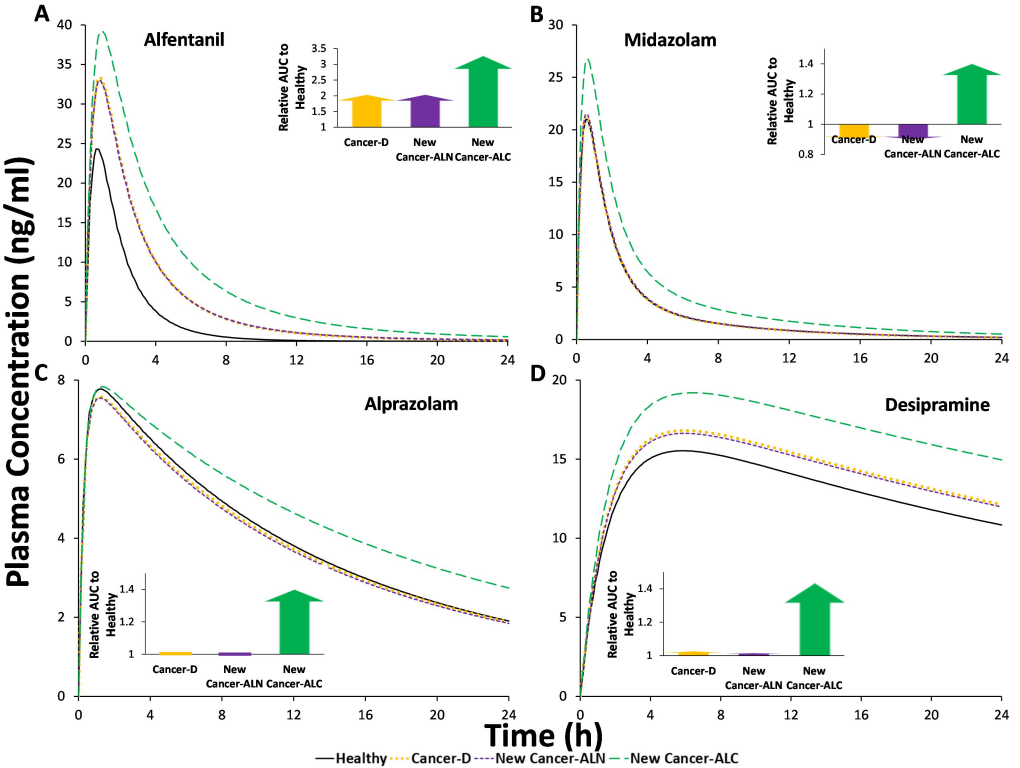
A
Alfentanil
Relative AUC to Healthy
Cancer-D
New Cancer-ALN
New Cancer-ALC
B
Midazolam
C
Alprazolam
D
Desipramine
Plasma Concentration (ng/ml)
Time (h)
Healthy
Cancer-D
New Cancer-ALN
New Cancer-ALC

Figure 6

Hepatic Scaling Factors for In Vitro-In Vivo Extrapolation (IVIVE) of Metabolic Drug Clearance in Patients with Colorectal Cancer with Liver Metastasis

Areti-Maria Vasilogianni, Brahim Achour, Daniel Scotcher, Sheila Annie Peters, Zubida M. Al-Majdoub, Jill Barber, Amin Rostami-Hodjegan

Drug Metabolism & Disposition

DMD-AR-2021-000359

Supplemental Information

Supplemental Table 1. Demographic and clinical details of CRLM patients.

Sample ID	Age at surgery (years)	Race	Sex	Body mass index, BMI (kg/m^2)	Smoking/ Alcohol use	Liver lobe	Diagnosis	Medical history	Treatment
389	52	Caucasian	Female	30.86	No/ Occasionally	Left	Metastatic moderately well differentiated adenocarcinoma	Deep vein thrombosis, asthma, duodenal ulcer, thyroid problem, liver lesions	Fragmin, levothyroxine, betamethasone, ventolin, ferrous fumarate
590	72	Caucasian	Male	32	Pipe/ 22 units per week	-	Metastatic moderate to Well differentiated adenocarcinoma (dirty necrosis)	Asthma, polypectomy, tonsillectomy, Hemicolectomy Dukes B	Salbutamol, tiotropium, lansaprozole, nasonex
633	67	Caucasian	Male	26.85	Ex-stopped/ -	Right	Metastatic adenocarcinoma & fatty liver disease	Peripheral neuropathy secondary to oxaliplatin, type 2 diabetes, hypercholesterolemia, valvular heart disease, prostate cancer with bone metastasis, colonic cancer T3N0, colorectal liver metastasis	Metformin, zoladex, oxaplatin and 5FU, irinotecan and 5FU with cetuximab
674	68	Caucasian	Female	26.67	No/ -	Right	Metastatic moderately differentiated adenocarcinoma	Rectosigmoid cancer 10/10 Dukes B	-
734	64	Caucasian	Female	23.84	No/ Occasionally	Right	Moderately to focally poorly differentiated metastatic adenocarcinoma	Primary colorectal	Dalteparin, short course of radiotherapy, adjuvant OXmdG and 5FU
746	85	Caucasian	Male	23.67	Ex (40 years)/ Moderately	Right	Metastatic papillary carcinoma	Laparoscopic R hemicolectomy T2M0, Squamous cell carcinoma (scalp), hypothyroidism, hypertension, Chronic	Irbesartan, levothyroxine, bisoprolol, aspirin, omeprazole, budesamide, formoterol

								obstructive pulmonary disease	
794	71	Caucasian	Female	22.41	No/ No	-	Metastatic adenocarcinoma with extensive intra-acinar necrosis	R hemicolectomy, pT3N2, high blood pressure, depression	Tomudex chemotherapy
818	58	Caucasian	Male	21.78	Ex (25 years)/ 18 units per week	-	Moderately differentiated metastatic adenocarcinoma	Sigmoid adenocarcinoma pT3pN2	Loperamide, carboplatin/5FU and modified de Gramont and radiotherapy
1492	34	-	Female	32.53	Ex-stopped/ Approximately 20 units per week	Right	Metastatic moderate and poorly differentiated adenocarcinoma	Bowel resection, pilonodal abcess x2, grometts (as a child), tonsillectomy (as a child), egg collection, occasional palpitations, asthma (as a child), reflux, joint problems in knees, treated for Irritable bowel syndrome	Omeprazole, amitryptyline, microgynon, glucosamine sulphate, ibuprofen, peppermint oil
1493	75	-	Male	-	No/ No	Right	Metastatic moderately differentiated adenocarcinoma	Sigmoid tumour, sleep apnoea, asthma	Cod liver oil, salbutamol inhaler, seretide inhaler, movicol
1498	63	Caucasian	Male	-	No/ Rarely	Right	Metastatic adenocarcinoma	Previous gout, anaemia, cataract operation	Doxycycline regime completed, Nil regular
1795	63		Male	36.32	Ex - stopped (previously 30cpd)/ Approximately 75 units per week	Left	Metastatic well differentiated adenocarcinoma	Adenocarcinoma, hypertension, intermittent claudication of left leg	Omeprazole, irbesartan, simvastatin, clopidogrel
1957	68	-	Male	32.16	No/ -	Left	Metastatic moderately differentiated adenocarcinoma	Primary rectal cancer, pneumonia post-operative, liver cancer, late lung metastasis	Nil regular

2036	43	-	Female	-	-/ -	Right	Metastatic moderate to poorly differentiated adenocarcinoma	Primary colorectal	Omeprazole, paracetamol
2058	79	Caucasian	Female	21.6	-/ -	Left	Metastatic adenocarcinoma	Below the knee amputation, primary colorectal, lung metastasis	Lansoprazole, ferrous sulphate, alendronic acid, paracetamol, codeine phosphate, senna, natecal D3
2095	55	Caucasian	Male	28.1	-/ -	Right	Metastatic moderately differentiated adenocarcinoma	Primary colorectal	Nil regular

Supplemental Table 2. Input parameters for PBPK modelling using Simcyp v18 R1 for alfentanil (predominantly metabolized by CYP3A4), alprazolam (predominantly metabolized by CYP3A4 and CYP3A5), desipramine (predominantly metabolized by CYP2D6), and midazolam (predominantly metabolized by CYP3A4 and CYP3A5).

Input Parameters				
Compound Name	**SV-Alfentanil**	**SV-Alprazolam**	**SV-Desipramine**	**Sim-Midazolam**
Mol Weight (g/mol)	416.520	308.800	266.400	325.800
log P	2.160	2.120	4.570	3.530
Compound Type	Monoprotic Base	Monoprotic Base	Monoprotic Base	Monoprotic Base
pKa 1	6.500	2.400	10.260	6.000
pKa 2	n/a	n/a	n/a	n/a
B/P	0.630	0.825	1.160	0.603
Haematocrit	45.000	45.000	45.000	45.000
fu	0.104	0.290	0.240	0.032
GI Absorption Model	1st order	1st order	1st order	1st order
GI Permeability Assay	n/a	n/a	Entered	n/a
GI Peff,man	Regional	Regional	Regional	Regional
Distribution Model	Minimal PBPK Model	Minimal PBPK Model	Minimal PBPK Model	Minimal PBPK Model
Vss (L/kg)	0.370	0.760	20.800	0.880
Prediction Method	Entered	Entered	Entered	Entered
Clearance Type	Enzyme Kinetics	Enzyme Kinetics	Enzyme Kinetics	Enzyme Kinetics
Trial Design				
Population Name	Sim-Healthy Volunteers/Cancer	Sim-Healthy Volunteers/Cancer	Sim-Healthy Volunteers/Cancer	Sim-Healthy Volunteers/Cancer
Use Pop Representative	No	No	No	No
Population Size	100.000	100.000	100.000	100.000
Number of Trials	10.000	10.000	10.000	10.000
No. of Subjects per Trial	10.000	10.000	10.000	10.000
Start Day/Time	Day 1, 09:00	Day 1, 09:00	Day 1, 09:00	Day 1, 09:00
End Day/Time	Day 2, 09:00	Day 2, 09:00	Day 2, 09:00	Day 2, 09:00
Study Duration (h)	24.000	24.000	24.000	24.000
Sampling Time	Pre-defined Uniform	Pre-defined Uniform	Pre-defined Uniform	Pre-defined Uniform
Sampling Site Selection	Off	Off	Off	Off
Prandial State	Fasted	Fasted	Fasted	Fasted
Route	Oral	Oral	Oral	Oral
Dose Units	Dose (mg/kg)	Dose (mg)	Dose (mg)	Dose (mg)
Dose	0.043	0.500	50.000	5.000
Start Day/Time	Day 1, 09:00	Day 1, 09:00	Day 1, 09:00	Day 1, 09:00
Dosing Regimen	Single Dose	Single Dose	Single Dose	Single Dose

Supplemental Table 3. Protein content (mg/g liver tissue) in homogenates, microsomes, and cytosols from histologically normal and cancerous tissues of CRLM patients.

	HomPPGL (mg/g liver tissue)																		
sample	**1957**	**818**	**1493**	**1498**	**389**	**734**	**746**	**1492**	**794**	**674**	**590**	**633**	**1795**	**2095**	**2058**	**2036**	**mean**	**SD**	**cv**
normal	119.5	150.2	167.9	144.1	83.4	266.7	107.4	156.7	75.1	107.6	109.1	135.7	120.2	104.2	84.4	86.0	126.1	46.7	0.37
tumor	138.2	89.5	92.0	104.9	184.9	37.1	64.6	70.4	86.6	204.8	77.0	63.7	42.0	43.0	47.3	43.7	86.9	50.2	0.58
	Uncorrected MPPGL (mg/g liver tissue)																		
sample	**1957**	**818**	**1493**	**1498**	**389**	**734**	**746**	**1492**	**794**	**674**	**590**	**633**	**1795**	**2095**	**2058**	**2036**	**mean**	**SD**	**cv**
normal	14.0	22.8	14.1	19.6	20.0	11.8	18.7	20.0	16.7	12.7	12.5	14.6	8.8	15.1	12.5	19.0	15.8	3.9	0.24
tumor	6.4	15.2	4.3	10.4	11.6	4.7	6.5	5.9	4.5	4.8	6.3	2.6	3.7	6.1	5.8	4.5	6.5	3.3	0.51
	CPPGL (mg/g liver tissue)																		
sample	**1957**	**818**	**1493**	**1498**	**389**	**734**	**746**	**1492**	**794**	**674**	**590**	**633**	**1795**	**2095**	**2058**	**2036**	**mean**	**SD**	**cv**
normal	43.4	67.8	32.3	47.7	55.6	34.1	76.1	70.8	75.6	77.1	41.2	47.0	33.9	80.7	57.7	58.7	56.2	16.9	0.30
tumor	54.6	67.2	39.9	58.6	54.1	54.8	41.5	29.4	29.2	24.8	50.9	33.8	30.8	32.1	41.1	31.3	42.1	12.9	0.31

Supplemental Table 4. NADPH cytochrome 450 reductase activities (units/mg tissue) in homogenates and microsomes from histologically normal and tumor tissues of CRLM patients.

	NADPH CYP450 reductase activity in homogenates (unit/mg)	NADPH CYP450 reductase activity in microsomes (unit/mg)	NADPH CYP450 reductase activity in homogenates (unit/mg)	NADPH CYP450 reductase activity in microsomes (unit/mg)
Sample ID	**Normal**		**Tumor**	
389	2.275	0.811	0.640	0.282
633	2.844	1.015	0.284	0.085
674	2.844	1.219	0.569	0.083
734	0.796	0.570	0.284	0.062
746	3.318	1.580	0.967	0.211
794	2.640	1.398	0.427	0.148
818	2.218	1.232	0.284	0.099
1492	3.270	1.708	0.640	0.165
1493	1.479	0.341	0.142	0.030
1498	2.275	1.719	1.422	0.708
1957	2.275	0.968	0.758	0.150
1795	1.479	0.513	-	-
2036	1.919	0.656	-	-
2058	2.275	0.704	-	-
2095	2.204	1.270	-	-
590	3.583	0.711	-	-
Mean	2.356	1.026	0.583	0.184
SD	0.73	0.44	0.37	0.19

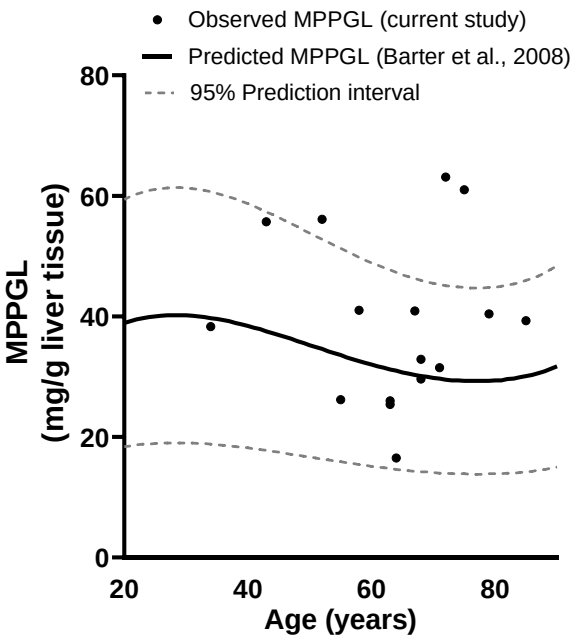

Figure S1. Relationship between observed (current study) and predicted MPPGL values and age (Barter et al., 2008), with 95% confidence intervals for the predicted values for Model 1. The observed MPPGL values correspond to the histologically normal samples.